ENERGETIC SOLAR ELECTRONS IN THE INTERPLANETARY MEDIUM

R. P. LIN

Space Sciences Laboratory, University of California, Berkeley, CA 94720, U.S.A.

Abstract. ISEE-3 measurements extending down to 2 keV energy have provided a new perspective on energetic solar electrons in the interplanetary medium. Impulsive solar electron events are observed, on average, several times a day near solar maximum, with ~40% detected only below ~15 keV. The electron energy spectra have a nearly power-law shape extending smoothly down to 2 keV, indicating that the origin of these events is high in the corona. These coronal flare-like events often produced ^{3}He-rich particle events.

In large solar flares which accelerate electrons and ions to relativistic energies, the electron spectrum appears to be modified by a second acceleration which results in a double power-law shape above ~10 keV with a break near 100 keV and flattening from ~10–100 keV. Large flares result in long-lived (many days) streams of outflowing electrons which dominate the interplanetary fluxes at low energies. Even in the absence of solar activity, significant fluxes of low energy electrons flow out from the Sun.

Solar type-III radio bursts are produced by the escaping 2–10^2 keV electrons through a beam-plasma instability. The detailed ISEE-3 measurements show that electron plasma waves are generated by the bump-on-tail distribution created by the faster electrons running ahead of the slower ones. These plasma waves appear to be converted into radio emission by nonlinear wave-wave interactions.

1. Introduction

Non-relativistic electrons from the Sun were first observed about two decades ago (Van Allen and Krimigis, 1965; Anderson and Lin, 1966). Measurements since then have shown that these electrons are the particle type most frequently emitted by the Sun (see Lin, 1974 for review). The University of California, Berkeley experiment (Anderson *et al.*, 1978) on the ISEE-3 (International Sun Earth Explorer) spacecraft has provided significantly improved measurements of 20 keV to several hundred keV electrons in the interplanetary medium, and more importantly, has provided for the first time high-sensitivity measurements extending to 2 keV. Since the range of such low energy electrons is significantly less than or comparable to the integrated straight-line path through the corona, these measurements can provide information on the location of the source region for these particles. Furthermore, at these energies the propagation of the electrons appears to be nearly scatter free, so the observed temporal profiles tend to reflect the variations at the solar source of these particles.

The observations generally show that the solar corona is a dynamic and perhaps continuous source of electron acceleration. Impulsive acceleration of electrons occurs, on average, several times a day or more, with most of these events unaccompanied by Hα flares. A large fraction of the impulsive electron events is observed only at energies below ~15 keV, and almost all these events appear to originate high in the corona. These coronal flare-like events often also produce ^{3}He-rich particle events. On the other hand, the large flare events which produce >10 MeV ion and relativistic electron acceleration, and which do not show ^{3}He enhancements, produce a significantly different shape of the electron spectrum. These large flares produce streams which last

Solar Physics **100** (1985) 537–561. 0038–0938/85.15.

for many days, during which the Sun appears to be a continuous source of low energy electrons. Interplanetary shocks and interplanetary type-III radio storms also produce long-lived streams.

Although the UCal particle experiment's period of operation in 1978–1979 was dominated by long-lived streams, there were a few periods of near constant quiet background. Even at these times, however, significant fluxes of low energy electrons were detected flowing out from the Sun.

Impulsive 2–10^2 electron events produce solar type-III solar bursts. The detailed ISEE-3 measurements extending to 2 keV have provided new insight into the emission mechanism for solar type-III radio bursts. Here we review progress in the above areas, concentrating on the ISEE-3 measurements.

2. Impulsive 2–10^2 keV Electron Events

Small non-relativistic solar electron events appear to be the most common type of impulsive particle emission from the Sun. Figure 1 shows an example of an impulsive solar electron event observed by ISEE-3. At the time of this event, the spacecraft was located in a halo orbit about the L1 Lagrange point about 10^6 km upstream of the Earth. This event is observed only at energies of 2–10 keV. ISEE-3 observations have shown that about 40% of the impulsive events (Table I) are observed only at energies below ~15 keV (Potter *et al.*, 1980).

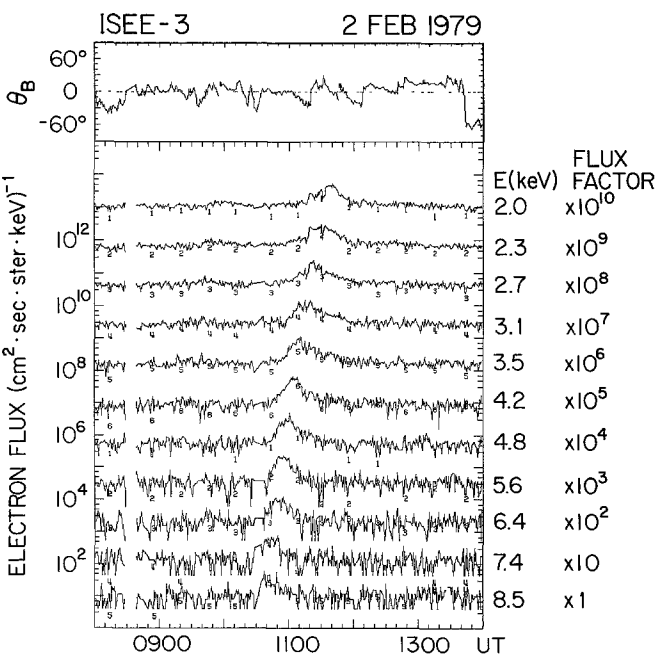

Fig. 1. An impulsive solar electron event observed by the ISEE-3 spacecraft. The top panel shows the angle of the interplanetary magnetic field direction to the ecliptic plane. The detector views ± 25° from the ecliptic plane.

TABLE I

Impulsive electron events

	2–10 keV only	> 15 keV	Total
Number of events:	136	190	326
with interplanetary type-III radio burst (30 kHz to 2 MHz)[a]	73/94	154/163	227/257
with metric/decametric type-III radio burst[b]	13/68	77/113	90/181
with reported Hα flare[b]	3/62	59/93	62/155
with 10 cm microwave burst[c]	1/(90)	42/(148)	43/(238)
with hard X-ray burst[d]	4/62	41/91	45/153

[a] Comparison with ISEE-3 radio experiments, J. Fainberg and R. G. Stone, private communication.

[b] From *Solar Geophysical Data.*

[c] From *Solar Geophysical Data*; the coverage is uncertain.

[d] Comparison with ISEE-3 solar X-ray experiment, S. R. Kane, private communication.

Several important characteristics are illustrated by this electron event. There is clear velocity dispersion with the fastest electrons arriving earliest, consistent with the simultaneous injection of the electrons at the Sun and nearly scatter-free propagation along the interplanetary Archimedean spiral field line to 1 AU. The rapid rise and decay at all energies confirms the lack of significant scattering. The electron distributions are

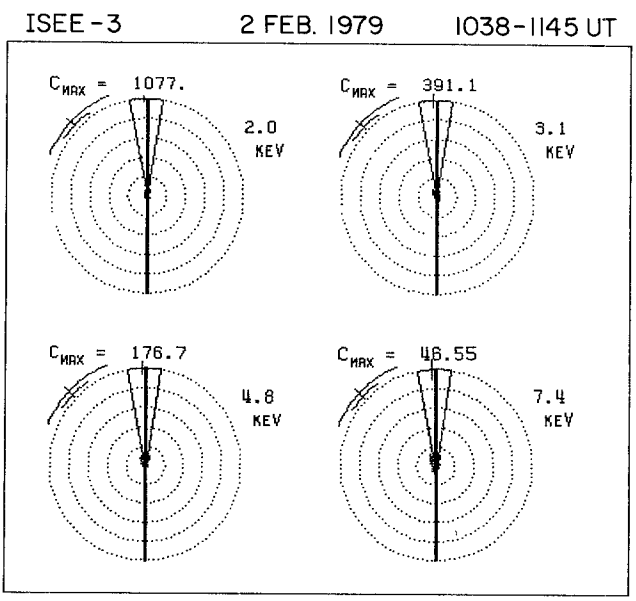

Fig. 2. 16-sector angular distribution of the electrons for the event of 2 February, 1979. Essentially all the counts fall into a single 22°5 sector.

highly anisotropic and beamed along the magnetic field (Figure 2) so dips in the electron fluxes are observed when the magnetic field swings out of the field of view of the detector.

There appears to be a transition at ~ 15 keV in the way electrons propagate in the interplanetary medium. Below this energy, adiabatic effects, especially focusing due to the decrease in the interplanetary field magnitude with distance away from the Sun, essentially always dominate over scattering to give nearly scatter-free propagation and beam-like angular distributions (Anderson *et al.*, 1981). Above ~ 15 keV, the electrons often show the diffusive time profiles and more broad angular distributions characteristic of scattering-dominated propagation.

The electron energy spectra for this event and several others are shown in Figure 3. These electron spectra extend smoothly down to 2 keV, although there are some departures from a power law spectral shape. Since low-energy electrons have a short range in the lower corona, the extension of the spectra to low energies implies that the

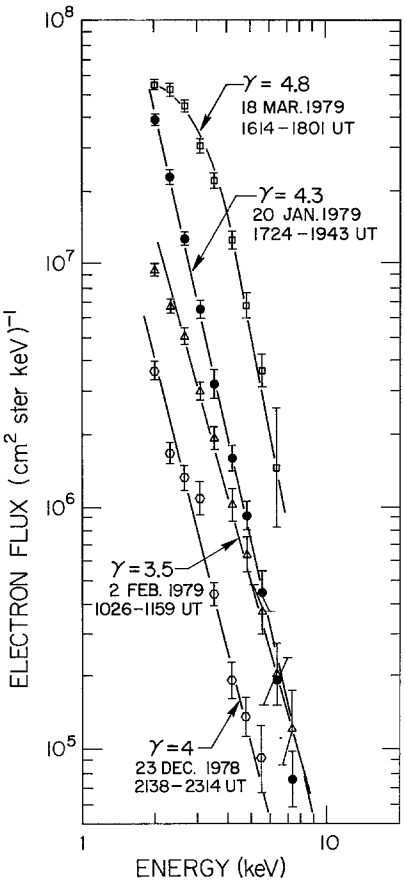

Fig. 3. Time-integrated energy spectra for several electron events (from Potter *et al.*, 1980). The spectra are fit to a power law, $dJ/dE \approx E^{-\gamma}$.

acceleration occurs high in the corona. To compute the effect of traversing the corona, we have used a coronal density model derived from radio measurements (Fainberg and Stone, 1974), and Trubnikov's (1965) expression for the energy loss of electrons in a hydrogen plasma. Starting with a power-law electron spectrum $dJ/dE \approx E^{-\gamma}$ with $\gamma = 4$ for an electron source located at varying heights, and assuming straight radially outward paths, we obtain the resultant spectra at 1 AU (Figure 4). Comparison with the observed spectra indicates that the electrons most likely are accelerated at altitudes greater than $0.5\ R_\odot$, although we cannot rule out the possibility that significant energy changes might have occurred for the electrons in their propagation from the Sun to 1 AU.

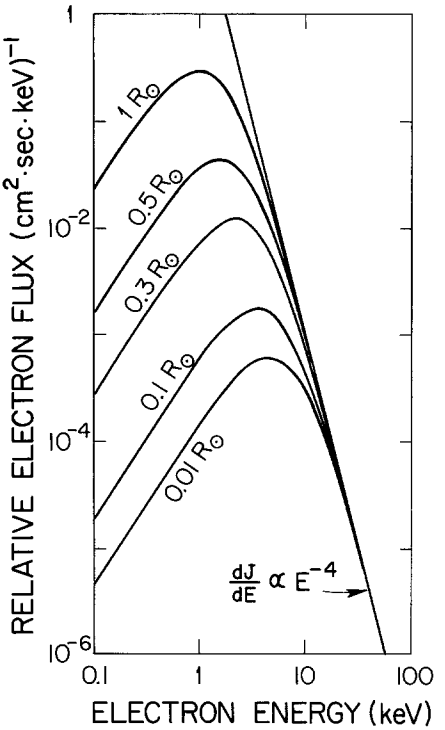

Fig. 4. Computed electron spectra at 1 AU resulting from injection of a $dJ/dE \approx E^{-4}$ power-law spectrum at different heights in the solar atmosphere (see text for details).

A total of 326 impulsive electron events were observed by ISEE-3 in the ~15 month period from August, 1978 to November, 1979. These events appear to fill typically ~60° in solar longitude in the interplanetary medium, so ~130 events/month must occur over the full Sun. Because the interplanetary medium is often filled with long-lived fluxes of electrons at these energies, small impulsive events will often not be detected. Thus the rate of occurrence of these events is probably significantly greater than estimated here.

About 40% of all the electron events (Table I) detected do not extend in energy above ~15 keV, but nearly all are observed to extend smoothly down to 2 keV, the limit of

the measurement. Almost all impulsive electron events are accompanied by a solar type-III radio burst observed in the interplanetary medium, i.e., at frequencies of ~ 30 kHz to a few MHz. On the other hand, only $\sim 50\%$ are associated with metric/decametric type-III bursts and a minority (40%) appear to have an associated Hα flare or microwave bursts at ~ 3000 MHz (18%). Comparisons with solar hard X-ray observations show that only 29% were associated with a detectable hard X-ray burst. The associations with solar phenomena are even poorer for the electron events observed only at 2–10 keV energies. These poor associations are consistent with the picture of many of these impulsive electron events, particularly those limited to 2–10 keV events, originating at heights of ~ 0.5–$1\ R_\odot$, without associated chromospheric activity. We have, therefore, called these events *coronal flares*. Based on the observed FWHM duration at 1 AU, the electron injection at the Sun occurs on time-scales of on the order of a few minutes. The total energy released into the interplanetary medium in electrons above 2 keV is estimated to be $\sim 10^{25}$–10^{26} ergs for these coronal flares. For those events where the electrons are observed at energies above ~ 15 keV, these $\gtrsim 2$ keV energy figures could increase by a factor of 10–10^2.

From the interplanetary observations alone, no clear division can be made between the events seen only in the 2–10 keV energy range and events which extend to energies above 15 keV. The > 15 keV events are more intense and more closely associated with the chromospheric Hα flares and hard X-ray bursts. In a study of one event where both hard X-ray emission and interplanetary electrons were detected, Pan *et al.* (1984) found that a model with energetic electrons accelerated in a region extending from the chromosphere to high in the corona was consistent with the observations. In this model, the low-energy escaping electrons come only from the upper part of the region, while high-energy electrons are able to escape from the entire region.

2.1. ^{3}He-RICH EVENTS

Recently, Reames *et al.* (1985) reported that virtually all solar ^{3}He-rich events are associated with impulsive 2 to 10^2 keV electron events. Solar ^{3}He-rich events (reviewed by Ramaty *et al.*, 1980) represent one of the most striking composition anomalies among the observed populations of solar and interplanetary energetic particles, with ^{3}He/^{4}He ratios of order unity, while the typical ratios for the solar atmosphere or solar wind are a few times 10^{-4} (Geiss and Reeves, 1972). The solar wind ^{3}He/^{4}He ratio varies but always remains below 10^{-2}, and it is uncorrelated with the occurrence of solar ^{3}He-rich events (Coplan *et al.*, 1983). Other properties of ^{3}He-rich events include reduced ^{1}H/^{4}He ratios and enhanced abundances of Fe and other heavy elements, and a tendency to larger ^{3}He enhancements in smaller events.

With the high sensitivity of the ISEE-3 energetic particle telescopes of the Goddard Space Flight Center experiment, it is possible to obtain temporal profiles with good resolution ($\lesssim 1$ hr) for the ^{3}He fluxes at ~ 1 MeV nucl.$^{-1}$ energy for the small ^{3}He-rich events. Figure 5 shows the 17 May, 1979 event where velocity dispersion can be seen in the ^{3}He fluxes. In the lower panel the associated 2–10^2 keV impulsive electron event with its velocity dispersion can be seen. The timing of the particle onsets and maxima

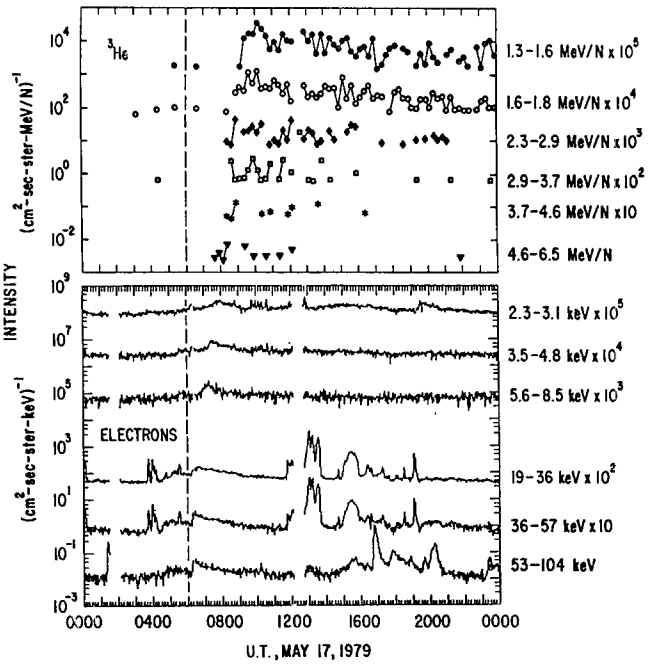

Fig. 5. Time histories of the intensities of ^{3}He and electrons of the indicated energy during 17 May, 1979 (from Reames *et al.*, 1985). The appearance of the plots differs partly because of the absence of continuous background fluxes for ^{3}He. The lowest isolated points for each energy of ^{3}He represent one particle per 15 min averaging period. The rapidly varying bursts (at ~04:00 UT and ~12:00 UT) observed in the higher, > 19 keV electron channels are due to particles from the Earth's bow shock. The 53–104 keV channel also responds to solar X-rays (~01:30, 16:30–20:30, and 23:30 UT). The dashed vertical line indicates the time of the type-III solar radio burst. Intensity scale factors are shown to the right of the energies.

are shown in Figure 6, where we have plotted those times versus $1/\beta$ (the particle velocity $v = \beta c$). If particles of all velocities were released at the same time t_0, and travelled the same distance L, their arrival times would be related by $t = t_0 + L/\beta c$, which would be a straight line on Figure 6. The observed onset time depends upon the relative instrument sensitivity, the rise time, and the event amplitude. The ^{3}He onsets lag the time that would be expected from the electron measurements by no more than about 10–15 min. The traversal distance implied by the onset time of the lowest velocity ^{3}He is ~1.3 AU. This compares with ~1.25 AU for the electrons. The times of maximum of ^{3}He are also consistenly later than those of electrons of the same velocity, implying a greater degree of scattering for ^{3}He in the interplanetary medium. The mean path lengths implied by the ^{3}He times of maximum are ~1.8–2.0 AU compared to ~1.45 AU for the electrons.

Energy spectra for the two species are shown in Figure 7. The spectral indices for the least-squares fits to a power-law are 2.7 ± 0.1 and 2.7 ± 0.3 for electrons and ^{3}He, respectively. For electrons, only the region from 2.3 to 60 keV was fit because of

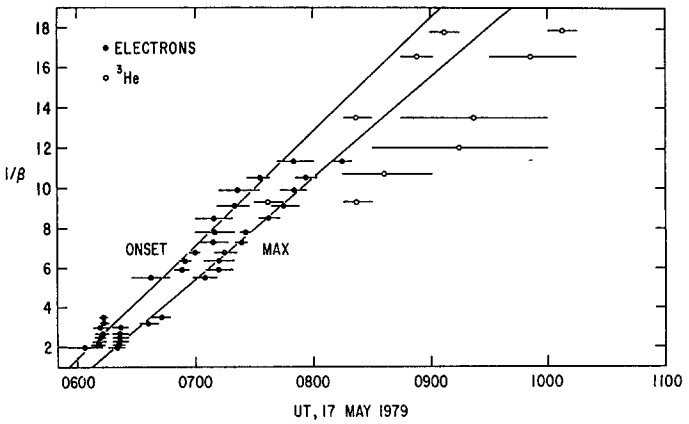

Fig. 6. Time of onset and peak flux for particles plotted versus $1/\beta$ where $v = \beta c$ is the particle velocity (from Reames *et al.*, 1985). The lines represent least-squares fits to the electron data only.

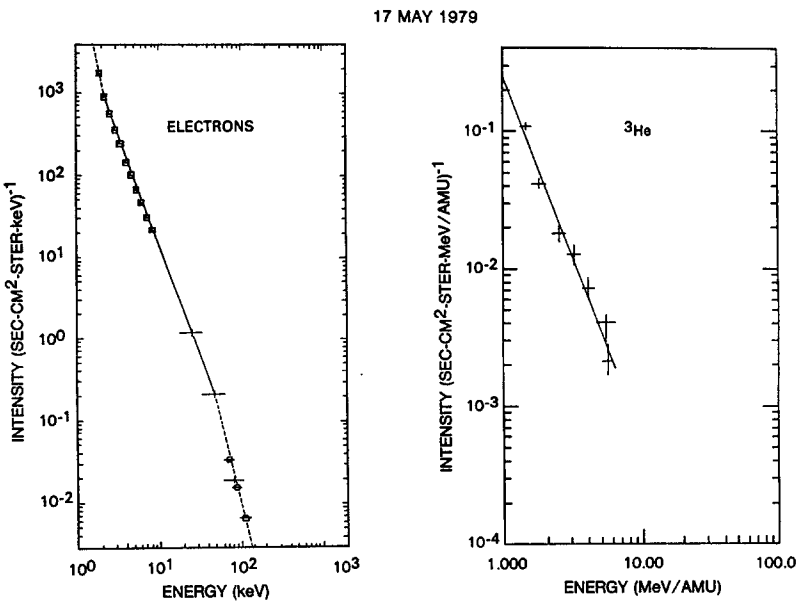

Fig. 7. Event-averaged energy spectra for electrons and ^{3}He in the 17 May, 1979 event (from Reames *et al.*, 1985). Lines through the data are least-squares fit lines to power-law spectra with resulting spectral indices 2.7 ± 0.1 for electrons and 2.7 ± 0.3 for ^{3}He. The electron fit was confined to the 2.5 to 60 keV region.

apparent spectral changes at higher and lower energies. Note that ^{3}He and electrons have the same spectral slope over ranges of comparable particle velocities.

In the 15-month interval in 1978–1979, about a dozen ^{3}He-rich events were observed with sufficient statistics to provide good temporal profiles. All of these events were accompanied by an impulsive 2–10^2 keV electrons with a temporal relationship similar to that shown in Figure 6. The solar associations for these ^{3}He-electron events are

essentially the same as for electron events in general: close association with kilometric wavelength type-III bursts, small Hα subflares or no reported Hα association, very few hard X-ray bursts, and small or no soft X-ray bursts.

The close temporal associations and similar spectral slopes suggest that the same acceleration process may be responsible for both electron and ^{3}He acceleration. A preliminary search indicates that ions of a few hundred keV total energy may also be accelerated at the same time as the ~ 1 MeV/nucl. ^{3}He and the electrons. These low energy ion fluxes are usually difficult to associate with an impulsive injection at the Sun because the travel time from the Sun to 1 AU is long, $\gtrsim 6$ hr, and the flux increases for ^{3}He events are small. Furthermore, there are many variations in the low energy fluxes on these same time-scales, due to local interplanetary effects. Even so, for many ^{3}He-electron events, there are increases in the few hundred keV ion fluxes at the right time for releases simultaneous with the electrons. At these energies we have no information on the composition of the ions.

Thus, 2–10^2 keV electrons, ~ 1 MeV/nucl. ^{3}He, and even lower energy ions may be accelerated together in coronal flare or flare-like events which occur at heights of 0.5–1 $R_\odot$. This type of acceleration differs from large flare events, where ions are accelerated to > 10 MeV energies and electrons to relativistic energies, with no ^{3}He enrichment observed.

3. Long-Lived 2–10^2 keV Electron Fluxes

The ISEE-3 spacecraft observes 2–10^2 keV electron fluxes to be present in the interplanetary medium at all times. Figure 8 shows the daily minimum flux in three energy intervals: 2–2.3 keV electrons, 19–45 keV electrons and protons (but primarily electrons), and > 272 keV protons. This type of plot excludes the impulsive electron events discussed above since their time scales are typically less than a few hours. It can be seen that these particle fluxes are dominated by streams which last many days. Many of these streams arise from a large solar flare event or series of such events from a single active region (Anderson *et al.*, 1982). Others appear to be dominated by the passage of an interplanetary shock (Tsurutani and Lin, 1985). Still others, generally lower intensity ones, appear to be related to type-III radio burst storms observed at hectometric and kilometric wavelengths (Bougeret *et al.*, 1985).

3.1. Large solar flares

Large solar flares are the most energetic natural particle accelerators found in the solar system, occasionally accelerating ions to tens of GeV and electrons to hundreds of MeV energies. Lin *et al.* (1982) presented IMP 6, 7, and 8 measurements of the energy spectrum of 20 keV to 20 MeV electrons observed from large solar flares (see Lin, 1974, and Simnett, 1974, for reviews of previous work). The aim of the study was to obtain information on the spectrum of the accelerated electrons at the Sun. To minimize propagation effects, only events from flares located at 30° to 90° W solar longitude were chosen for study. The energy spectra were constructed using the maximum flux observed

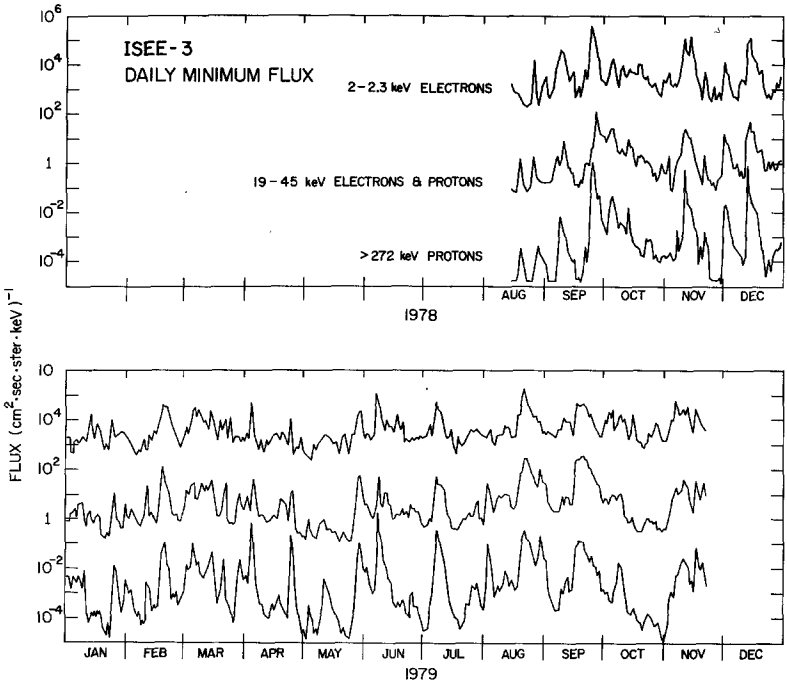

Fig. 8. Plotted here at the minimum flux levels for each day for 2–2.3 keV electrons, 19–45 keV electrons and protons, and >272 keV protons, for August, 1978 to November, 1979. The fluxes are dominated by long-lived streams, but even at the quietest times there are significant fluxes of electrons.

at each energy. These spectra were shown to be representative of the spectra of the electrons escaping from the Sun over this range of energies. Figure 9 shows the large solar flare event of 25 November, 1971. Terrestrial particle fluxes at energies $\lesssim 100$ keV are present from ~ 1030 onward but are not significant at the event maximum near 10:00 UT. Figure 10(a) shows the energy spectrum. A flat power law spectrum is observed below ~ 100 keV, changing to a much steeper power law at higher energies. Figure 10(b) shows the spectrum for the large event of 30 April, 1973, where the spectrum extends to ~ 20 MeV. In this case, the data at $\geqslant 10$ MeV are a factor of more than 5 below an extrapolation of the 0.2 to 2.0 MeV spectrum, providing clear evidence for a steepening of the spectrum at very high energies. It was found that every event shows the same spectral shape: a double power law with a smooth transition around 100–200 keV and power law exponents of 0.6–2.0 below and 2.4–4.3 above. The more intense the event, the harder the spectrum observed. In some cases, the spectra are observed to steepen above 3 MeV.

Lin *et al.* (1982) also investigated whether the ions which are accelerated in the same large flares have a similar characteristic spectrum and whether that spectrum is related to that of the electrons. Van Hollebeke *et al.* (1975) found that proton spectra in the $\sim$ 10–80 MeV range generally fit well to a power law. Figure 11 gives the best fit proton power-law spectral index in the >10 MeV energy range versus the low energy

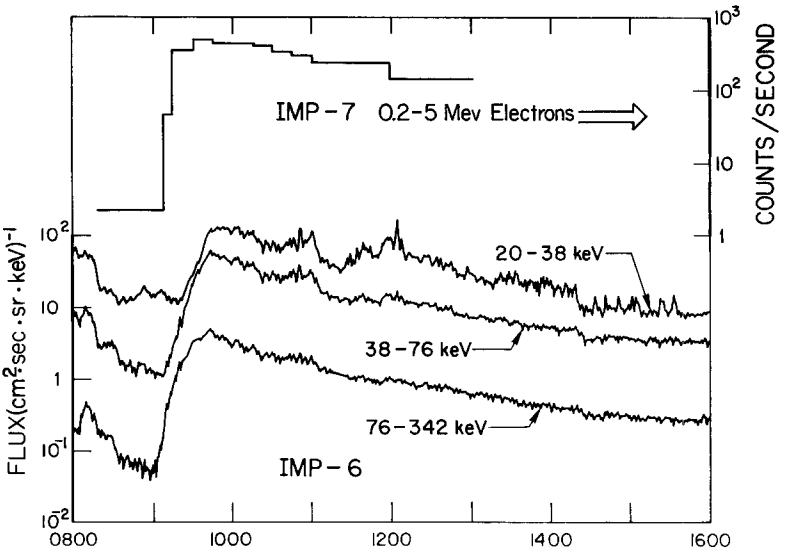

Fig. 9. The 25 November, 1977 solar electron event (from Lin *et al.*, 1982). Upstream terrestrial particles are present at IMP 6 prior to the event onset at ~09:00 and also sporadically between ~10:30 and 15:30 UT.

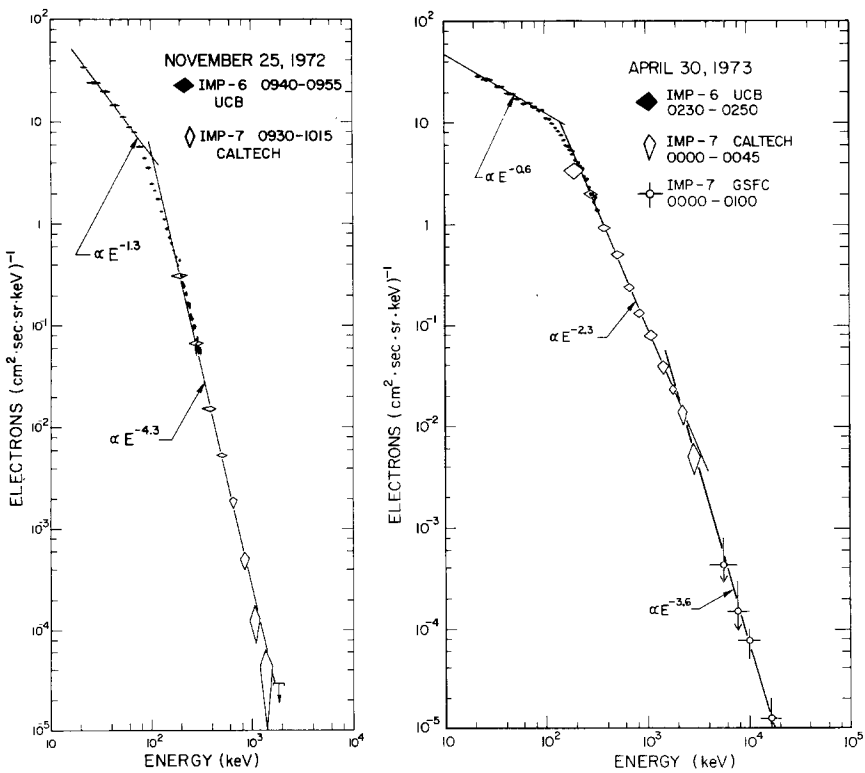

Fig. 10. The energy spectra for the 25 November, 1972 and 30 April, 1973 events (from Lin *et al.*, 1982). Both events show a smooth transition between ~100 and 200 keV. Some steepening is observed above ~3 MeV for the April event.

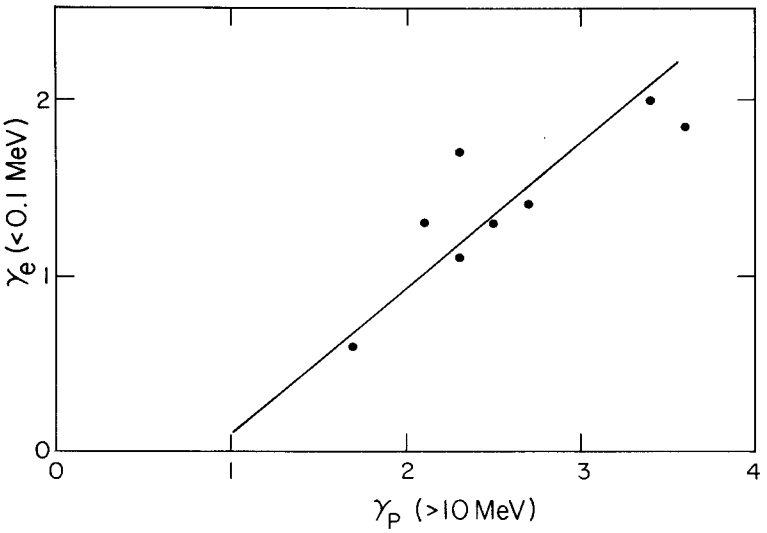

Fig. 11. Plotted here is the electron spectral exponent in the range 10–100 keV vs the proton spectral exponent in the 10–80 MeV range, for well connected large flare events observed by IMP 6, 7, and 8 (from Lin *et al.*, 1982).

<0.1 MeV electron spectral index for eight of the events. As can be seen, the electron and proton spectra appear correlated. Comparisons with the high energy >0.2 MeV electron spectral indices, however, yield little, if any, correlation. It may be significant that 10–80 MeV protons have approximately the same velocities as 5–40 keV electrons.

The spectral correlation in Figure 11 suggests that the electrons and protons are accelerated by the same mechanism. For velocity dependent acceleration, the break in the electron spectra at 100–200 keV would imply a similar break at $\sim$200–400 MeV for protons. Although a characteristic sharp break has not been reported for protons at these energies, steepening of the spectra at a few hundred MeV is often observed (Fichtel and McDonald, 1967).

The observed escaping electron spectra are generally consistent with the hard X-ray spectra typically observed from large flares. Recently, detailed high spectral resolution ($\lesssim 1$ keV FWHM) measurements of an intense solar hard X-ray burst on 27 June, 1980 showed that the hard X-ray emission was well fit by a double-power-law spectral shape with break energies of $\sim 10^2$ keV (Schwartz, 1984; Lin, 1984). Single power law shapes and emission from an isothermal plasma could be excluded.

Hard X-ray bursts for large flares have systematically much harder X-ray spectra, power-law indices of $\gamma_x < 2$–3 below 100 keV, than typical small flares ($\gamma_x \gtrsim 4$). For the 4 August, 1972 large flare, a break to a steeper power-law spectrum above ~ 100 keV energies was observed in the hard X-ray spectrum (Hoyng, 1975). This X-ray break implies a break in the bremsstrahlung producing electrons at ~ 140 keV (Ramaty *et al.*, 1975). A similar break at ~ 100 keV is reported in the X-ray spectrum for an over the limb flare event on 22 July, 1972 (Hudson *et al.*, 1981), and during the impulsive phase of the 30 March, 1969 large flare (Frost and Dennis, 1971). The reported X-ray

power-law indices correspond to electron spectral indices consistent with those obtained from interplanetary measurements.

ISEE-3 provides the first measurements of the electron spectrum below ~ 20 keV for large solar flares. Figure 12 shows the electron spectrum from 2 keV to ~ 1 MeV for the

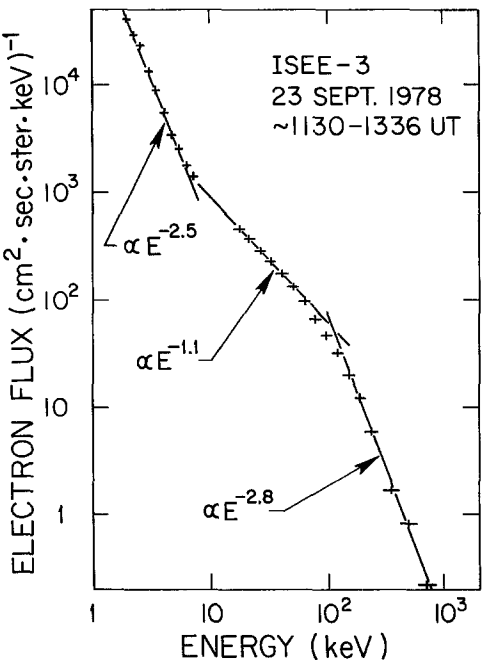

Fig. 12. The energy spectrum for the large solar flare event of 23 September, 1978 as observed by ISEE-3.

large solar flare of 23 September, 1978. The characteristic double-power-law shape with a break near $\sim 10^2$ keV and flattening below is observed. Below ~ 10 keV, however, the spectrum breaks upward again, with a power law index similar to that at energies above $\sim 10^2$ keV. Although the propagation of these lower energy $\lesssim 10$ keV electrons is nearly scatter-free while the $\gtrsim 20$ keV electrons propagate more diffusively, this difference is unlikely to produce a spectral change as large as observed here. We believe that this spectral break near ~ 10 keV reflects a real break in the injection spectrum at the Sun.

The electron spectra for small flare or coronal flare events tends to be smooth and free of breaks in the ~ 10 keV region. The spectra for large flare events suggests that a second acceleration occurs in large flares which accelerate both ions and electrons to MeV energies and above. This second acceleration appears to pick up electrons above ~ 10 keV in energy and accelerate them further. Solar flare gamma-ray observations from the Solar Maximum Mission (SMM) spacecraft indicate that if there is a physically distant second acceleration process in large flares, it must occur within seconds of the initial impulsive electron acceleration in some large flares (Chupp, 1983).

This second acceleration may be produced by the flare shock wave as it passes through the solar corona. The spectra observed here may be characteristic of the collisionless shock acceleration process. We note that flare shock waves in the interplanetary medium near 1 AU, corotating shock waves in the distant heliosphere, and bow shocks in front of planetary magnetospheres all accelerate particles to similar spectral shapes (Lin, 1980), although the energy ranges and flux levels are vastly different.

Large solar flare electron events decay away rapidly at high energies (see Figure 9). At low energies, however, enhanced electron fluxes persist in the interplanetary medium for many days following a large solar flare (Anderson *et al.*, 1982). The angular distribution for these long-lived electron fluxes still appears to be dominated by adiabatic effects (Anderson *et al.*, 1981) with a strong net outflow. Thus it appears that a long-lived source of particles is created near the Sun by these large flares and/or their associated active region. This source region supplies interplanetary magnetic field lines over a wide range of heliographic longitudes for many days. It is not known whether this long-lived source results from storage of particles from the large flare high in the corona or from continued acceleration in the high corona. The spectral shape of the low-energy electrons, however, stays a power law down to ~ 2 keV throughout the stream without significant variation in slope.

In some instances, the initial large flare impulsive event is not observed, but the flare-associated interplanetary shock is observed by ISEE-3, superimposed on a slowly rising long-lived stream. The interplanetary shock is commonly observed to accelerate electrons locally at energies below ~ 10 keV (Potter, 1981; Tsurutani and Lin, 1985), in contrast to the situation at energies > 20 keV, where shock acceleration is only very rarely observed to have any effect.

3.2. Interplanetary type-III storms

Besides the streams produced by large solar flares and interplanetary shocks there are many less intense long-lived streams which appear to be related to interplanetary type-III radio storms (Fainberg and Stone, 1970). These storms consist of thousands of type-III radio bursts emitted per day at frequencies of from a few MHz to tens of kHz, corresponding to a height range of ~ 10 solar radii to 1 AU. They last from 1 to 12 days and up to 3 storms are observed per solar rotation. An average of ~ 25 storms per year occurred in 1978–1982 (Fainberg *et al.*, 1982). The storms correlate with type-I and type-III radio storms observed at higher frequencies.

These interplanetary radio storms are usually associated with long-lived streams of electrons which show little, if any, impulsive features (Bougeret *et al.*, 1985). Apparently impulsive injections of electrons are so frequent in a storm that the fluxes from individual injections are washed out by the time the electrons reach 1 AU. The energy spectrum of these storm-related stream electrons appears similar to that observed for impulsive solar electron events, and the peak electron fluxes are usually significantly lower than for large flares or interplanetary shocks.

3.3 QUIET-TIME ELECTRONS

In 1978–1979, close to solar maximum, there are only a few short periods when the interplanetary medium appears to be free of long-lived streams associated with solar activity. At these times it may be possible to detect the quiet-Sun emission of suprathermal electrons. Figure 13 shows the spectrum of electrons at one of the quietest times

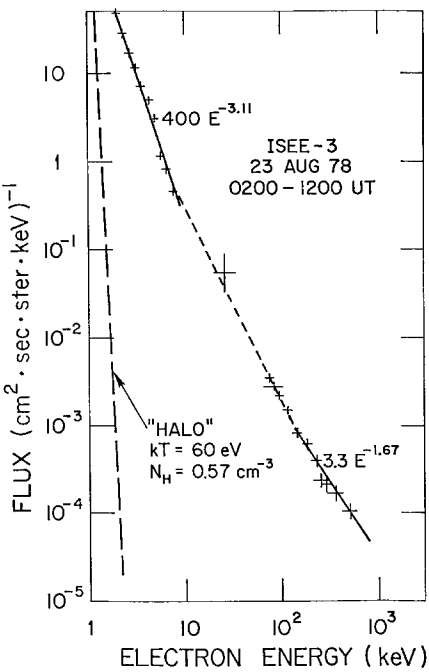

Fig. 13. The electron spectrum at an apparent quiet time. An extrapolation of the typical solar wind halo electron spectrum (Feldman *et al.*, 1975) is shown for comparison.

in the 15-month period of observations. The electron fluxes were decaying from a stream dominated by an interplanetary shock on 18 August, but had bottomed out by ~2200 UT, 22 August. During the 0200–1200 UT period of this spectrum the 2–10 keV electron fluxes were very stable and still flowing out away from the Sun, although the anisotropy was small. The energy spectrum is characterized by a power law with spectral slope about -3, similar to that observed in long-lived streams. Shown for comparison at low energies is the extrapolation of the solar wind halo electron population (Feldman *et al.*, 1975) which can be characterized by a temperature of $kT \sim 60$ eV. Even at this quiet time the observed electron fluxes at >2 keV energies are many orders of magnitude above the solar wind population. Thus the Sun appears to be a continuous source of

non-thermal electrons at energies above ~ 2 keV. The mechanism for producing this non-thermal population is unknown; perhaps these electrons are a byproduct of the coronal heating mechanism or possibly the escaping electrons from hard X-ray microflares (Lin *et al.*, 1984).

At energies from ~ 10 keV to ~ 200 keV the electron may also be of solar origin but the measurements are more dominated by instrument background. At energies above a few hundred keV the spectrum appears to have the same spectral slope as observed for the interplanetary electrons from Jupiter. These Jovian electrons are known to dominate the quiet-time interplanetary electron fluxes above a few hundred keV (Teegarden *et al.*, 1974).

4. Solar Type-III Radio Bursts

Table I shows that impulsive electron events are essentially always accompanied by solar type-III radio bursts observed at hectometric and kilometric wavelengths. With the sensitivity of the UCal ISEE-3 particle experiment, the number of impulsive electron events detected is now comparable to the number of discrete type-III radio bursts observed at hectometric and kilometric wavelengths, provided the limited ($\sim 60°$) longitudinal range of the electron events is taken into account.

Type-III radio emission is produced by ~ 2–10 keV electrons impulsively accelerated at the Sun. As these electrons escape from the Sun, the faster ones will run ahead of the slower ones to produce locally a bump-on-tail velocity distribution. Electron plasma (Langmuir) waves are then excited at the local electron plasma frequency via the two-stream instability (Bohm and Gross, 1949). Electron plasma waves with phase velocities corresponding to the positive slope portion of the bump will grow at the expense of the free energy in the bump. If the plasma waves grow rapidly enough, the bump should be flattened out, a process known as 'quasi-linear relaxation' or 'plateauing'. For a spatially homogeneous beam-plasma model the fast particle beam is so rapidly diffused in velocity space by the intense plasma oscillations that a coherent stream would only be able to travel a few kilometers from its source before it is plateaued (Sturrock, 1964). For type-III bursts, however, the beam is spatially inhomogeneous, and velocity dispersion will tend to reform the bump that quasi-linear plateauing has flattened. Also, plasma waves produced with a given phase velocity may later be reabsorbed by the electron stream when the bump goes to lower velocities. A number of numerical computations of the quasi-linear evolution of the electron stream, and growth and reabsorption of the plasma waves, have been done (Takakura and Shibahashi, 1976; Magelssen and Smith, 1977; Grognard, 1982), which show that the stream will be able to propagate out at least to distances on the order of an astronomical unit. These numerical models predict electron distributions which are very plateau-like, and plasma wave levels which sometimes exceed the threshold for strong turbulence effects to become important (Nicholson *et al.*, 1978; Goldman, 1983).

Both the plasma waves (Gurnett and Anderson, 1976, 1977) and electrons (Lin, 1970, 1974; Frank and Gurnett, 1972; Lin *et al.*, 1973) associated with type-III bursts

have now been detected *in situ* at 1 AU. Figure 14 shows an impulsive electron event with associated type-III radio emission and *in situ* electron plasma waves (Lin *et al.*, 1981). The top panel shows the electric field intensities in four frequency channels from 17.8 to 100 kHz. The smooth intensity variations characteristic of a type-III radio burst, consisting of a rapid rise followed by a slow monotonic decay, are clearly evident in the 56.2 and 100 kHz channels.

The very intense irregular electric field intensity variations in the 31.1 kHz channel from about 20:00 to 21:30 UT are narrow band electron plasma oscillations. Because of the filter overlap, somewhat weaker electron plasma oscillation intensities are also evident in the 17.8 and 56.2 kHz channels.

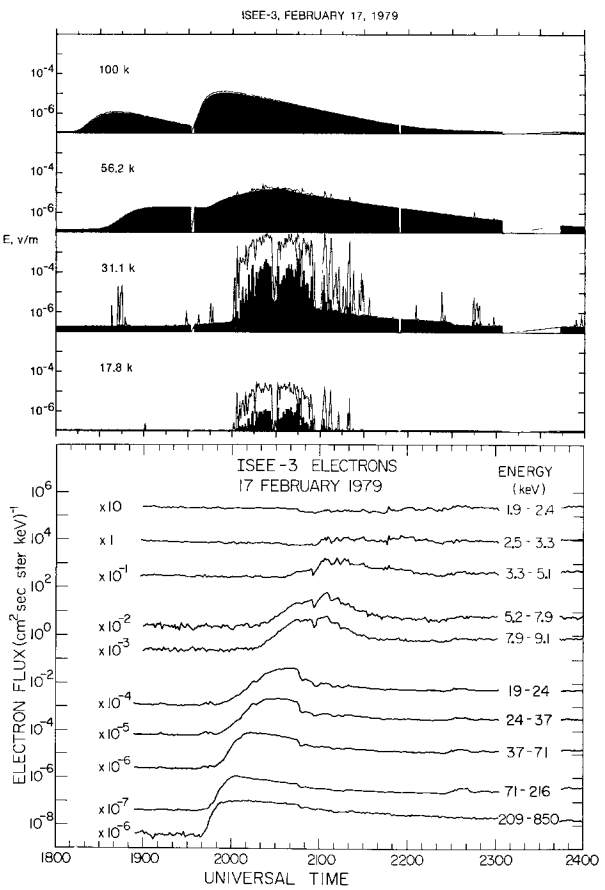

Fig. 14. The top panel shows the electric field intensity measured from ISEE-3 (from Lin *et al.*, 1981) on 17 February, 1979 in four broad frequency bands for the event of interest. The black areas show the intensity averaged over 64 s. The solid lines give the peak intensity measured every 0.5 s. The smoothly varying profiles in the 100 and 56.2 kHz channels show two solar type-III radio bursts. The second one is of interest here. The intense highly impulsive emissions observed in the 31.1 and 17.8 kHz channels are the plasma waves. The lower panel shows the omni-directional electrons from 2 keV to >200 keV. The velocity dispersion is clearly evident. No significant increase is observed below ~2.5 keV.

The large difference between the peak and average electric field intensities indicates that the plasma oscillations are very impulsive. The peak amplitudes appear to be limited to a level of a few mV m^{-1}. These very impulsive fluctuations are characteristic of previous observations of electron plasma oscillations associated with type-III radio bursts. Although more intense bursts have been observed closer to the Sun, this is one of the most intense plasma oscillation events observed at 1 AU.

The bottom panel of Figure 14 shows the spin-averaged low-energy electron intensities simultaneously detected by ISEE-3. The solar flare electrons are first detected above 200 keV energy at about 19:40 UT. Electrons are subsequently detected in progressively lower and lower energy channels at later and later times with very clear evidence of velocity dispersion. Simple comparison of the plasma wave and electron intensities suggests that the plasma oscillations are clearly associated with electrons in the energy range of about 3 to 30 keV.

Figure 15 shows the first measurements from ISEE-3 of the reduced (integrated over perpendicular velocities) parallel velocity distribution functions for the fast electrons associated with a type-III radio burst at 1 AU. The solid dots in Figure 15(a) show $f(v_{\|})$ for the background population just prior to the onset of the electron event. This type of background population of non-thermal electrons is observed at all times, although at varying flux levels. The level of this long non-thermal tail background population is important in determining when a bump will be formed in the distribution. Figure 15 shows $f(v_{\|})$ every 5 min for the event 19:45–21:55 UT). Each succeeding distribution is shifted to the right by 2×10^9 cm s^{-1} in velocity. The electron distributions develop a well-defined bump-on-tail with the bump progressing to lower velocities with time. In contrast to the expectations of quasi-linear models, however, there is no obvious plateauing of the bump; at a given phase velocity significant positive slopes persist for many minutes. The evolution of the observed Langmuir waves is qualitatively consistent with the variations of the electron distribution, but the wave levels are substantially below the levels predicted from the electron distributions. These measurements indicate that the Langmuir waves were being shifted out of resonance with the electron beam.

Various nonlinear wave-wave interactions have been suggested for shifting the plasma waves out of resonance with the electron beam (see Goldman, 1983, for review). These include induced scattering of the Langmuir waves off ion clouds (Kaplan and Tsytovich, 1968), parametric instabilities such as oscillating two-stream instability (Papadopoulos *et al.*, 1974) and strong turbulence processes such as soliton collapse (Zakharov, 1972; Nicholson *et al.*, 1978). In general, the dominant Langmuir wave transfer processes are those which involve a low-frequency excitation in addition to another Langmuir wave (Tsytovich, 1970). For example, induced scattering, which occurs when $T_e \approx T_i$, can be viewed as the process of decay of the initial or pump Langmuir wave into an acoustic wave which is heavily damped, and another Langmuir wave (Bardwell and Goldman, 1976). For $T_e > T_i$, the ion acoustic wave is more weakly damped and this process becomes the parametric decay of the initial Langmuir wave into an ion acoustic wave and a daughter Langmuir wave.

Density irregularities and ion acoustic waves already present in the solar wind can

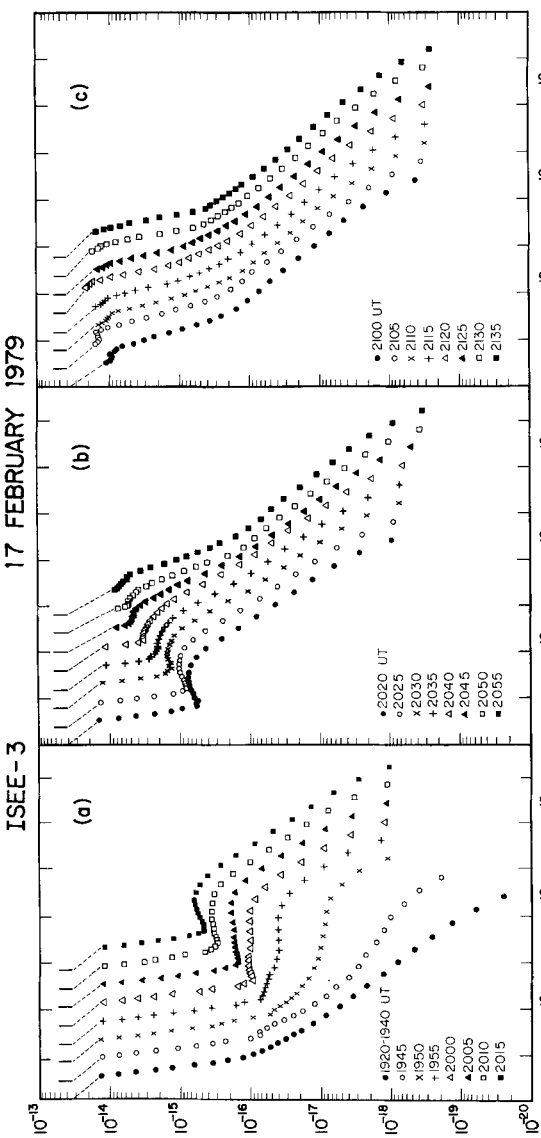

Fig. 15. The comprehensive measurements over energy and angle taken from ISEE-3 on 17 February, 1979 heve been used to construct the one-dimensional velocity distribution function of the electrons every 64 s (from Lin *et al.*, 1981). The distribution averaged over 20 min prior to the event onset is indicated by the solid dots in panel (a). The 64 s measurements of the distribution during the event are shown every five minutes. Note the positive slope which develops and moves to lower velocities with time. During the interval ~ 20:45-20:55 UT the measurements are incomplete because the magnetic field is not contained in the electron detectors' field of view. After 21:00 UT positive slopes are only infrequently observed in the distribution.

also significantly affect the growth and saturation of beam-driven Langmuir waves, to the point of stabilizing the beam (Escande and de Genouillac, 1978; Goldman and DuBois, 1982; Russell and Goldman, 1983).

Lin *et al.* (1985) searched for low frequency fluctuations in association with the

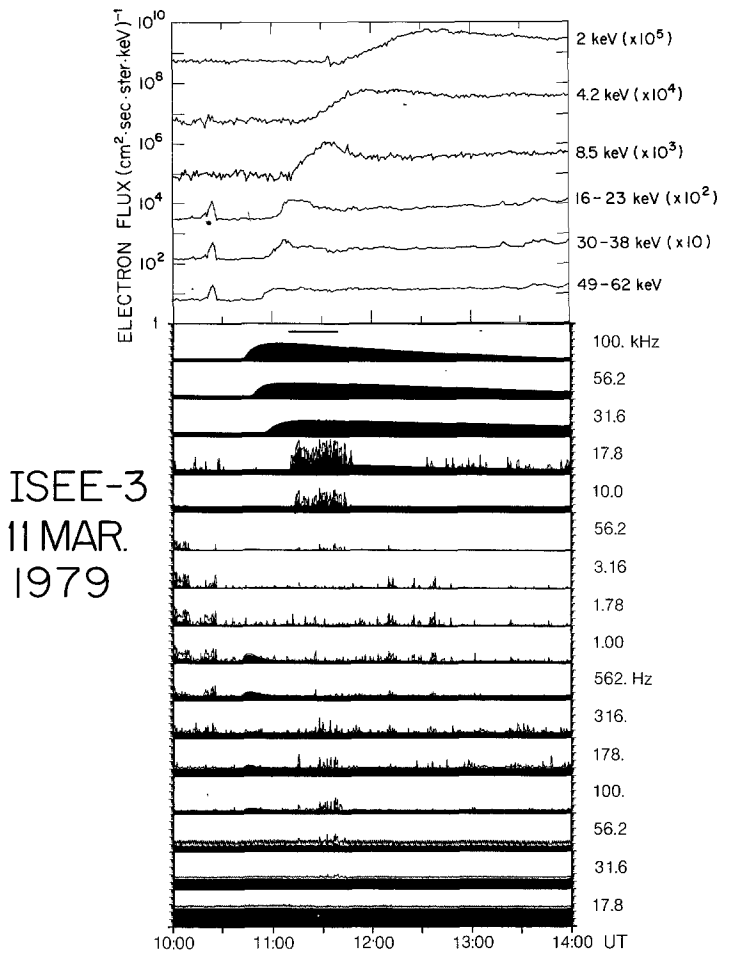

Fig. 16. The top panel shows the spin-averaged flux of electrons from 2 to 62 keV for the type-III solar radio burst of 11 March, 1979. The spike at 10:20 UT and smaller spikes which occur simultaneously in several energy channels are due to energetic particles flowing upstream from the Earth's bow shock. Velocity dispersion is clearly evident for the solar electrons. The lower panel shows the electric field intensity measured in 16 broadband channels from 100 kHz down to 17.8 Hz. The horizontal bar at the top indicates times of positive slope in the electron reduced velocity distribution $[f(v_\parallel)]$. The black areas show the average intensity over 32 s. The solid lines give the peak intensity. The smoothly varying profiles (100, 56.2, and 31.6 kHz) show the type-III radio burst. The intense, highly impulsive emissions at 17.8 kHz and 10 kHz are electron plasma waves. The sporadic bursty emissions between 3.16 kHz and ~316 Hz have been previously identified as short wavelength ion acoustic waves. The impulsive emissions at frequencies from 316 to 31.6 Hz which occur from ~11:15 to 11:45 UT, simultaneous with the electron plasma waves, are believed to be long wavelength ion acoustic waves (from Lin *et al.*, 1985).

Langmuir waves observed in type-III radio bursts by the ISEE-3 spacecraft. Figure 16 shows a type-III solar radio burst with clearly associated Langmuir waves and energetic electrons, in the format similar to that for Figure 14. For this event $f(v_\parallel)$ exhibits a bump-on-tail from 1109 to 11:42 UT.

The bottom panel of Figure 16 shows the electric field intensities in sixteen frequency channels from 17.8 Hz to 100 kHz. The smooth intensity variations characteristic of a type-III radio burst, consisting of a rapid rise followed by a slow monotonic decay, are clearly evident in the 31.6, 56.2, and 100 kHz channels. The electron plasma oscillations are observed in the 17.8 kHz channel from about 11:10 to 11:50 UT, in good temporal agreement with $f(v_\parallel)$. From ~ 316 Hz down to 31.6 Hz there are highly impulsive bursts at the same time as the most intense bursts of Langmuir waves. In the 56.2 and 31.6 Hz channels, these are the only bursts detectable above the background.

Figure 17 presents plots of the highest time resolution (0.5 s) data of the wave instrument for the 17.8 kHz Langmuir wave channel and the 100 Hz electric field channel for the period 11:36–11:40 UT. The Langmuir waves are extremely impulsive: intensity changes of over two orders of magnitude can occur within 0.5 s and single bursts rarely last more than one or two 0.5 s readouts. Most, but not all, of the Langmuir bursts which exceed ~ 0.1 mV m^{-1} are accompanied by a corresponding burst at 100 Hz. The maximum electric field at ~ 100 Hz is ~ 0.04 mV m^{-1}, almost two orders of magnitude above the background level. The fact that this low frequency noise is not observed in the 100 Hz magnetic channel suggests that it is a low-frequency electrostatic mode, most likely a long wavelength ion-acoustic wave.

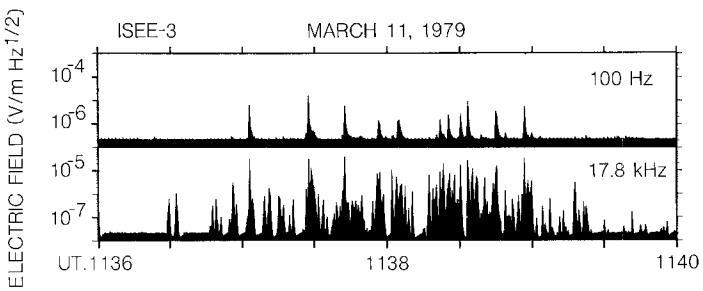

Fig. 17. High time resolution (0.5 s) plots of the Langmuir wave channel (17.8 kHz) and the 100 Hz long wavelength ion acoustic wave channel for the 11 March, 1979 event (from Lin *et al.*, 1985). Note the close correspondence between the most intense Langmuir wave spikes and the 100 Hz spikes.

The close temporal correlation of the 30–300 Hz low frequency noise bursts with the most intense Langmuir wave bursts suggests that they are the result of some nonlinear wave-wave interaction. Theoretical work and numerical simulations suggest that strong turbulence phenomena such as modulational instability and self focusing of Langmuir waves (soliton collapse) should become important at a threshold of $W = E^2/8\pi nkT_e \approx 10^{-5}$, where E is the Langmuir wave electric field (see Goldman, 1983, for review). Almost all the type-III events observed at 1 AU, however, have

maximum values of W substantially below 10^{-5}. Although very intense plasma waves confined to very small spatial regions, such as might be expected for soliton collapse, might be missed by the plasma wave instrument, it appears that, with the possible exception of a few very intense events (such as the 17 February, 1979), it is unlikely that strong turbulence phenomena play a significant role in type-III bursts.

The obvious interpretation of the low frequency, 30–300 Hz, noise observed simultaneously with type-III Langmuir wave bursts is that it is due to long wavelength ion acoustic waves. Because the typical $T_e/T_i \approx 4$, these ion-acoustic waves are not very strongly damped so a parametric decay instability, rather than induced scattering, might be appropriate to the situation for type-III radio bursts observed at 1 AU.

Two three-wave decay processes appear relevant: the decay of a pump Langmuir wave into a daughter Langmuir wave and an ion acoustic wave, $L \rightarrow L' + I$; and into a daughter transverse electromagnetic wave and an ion acoustic wave, $L \rightarrow T + I$. Based on preliminary analysis, it appears that the threshold is exceeded by the observed Langmuir wave levels only for the latter process. The transverse waves from this latter decay process would provide a natural source for type-III radio burst emission at the fundamental, i.e., near f_{p-}.

In the 17 February, 1979 event the radio emission at frequencies near the harmonic, $2f_{p-}$, which was believed to originate near the spacecraft because of its lack of directivity, actually began some 20 min *prior* to the onset of the Langmuir waves which were supposed to produce the radio emission. Lin *et al.* (1981) pointed out that this difficulty could be resolved if what was identified as harmonic radiation produced *in situ* could instead be fundamental radiation produced much closer to the Sun (see Kellogg, 1980). Significant scattering of the fundamental radio emission off density irregularities would be required to explain the lack of directivity. Evidence that fundamental emission dominates from burst onset to peak, and that scattering is important in the interplanetary medium, has recently been presented (Dulk *et al.*, 1985; Steinberg *et al.*, 1985).

5. Summary

Figure 18 summarizes the observations of electrons in the interplanetary medium. At energies above $\sim 10^9$ eV the galactic cosmic-ray electron component has essentially unattenuated access into the heliosphere (lower left corner). From $\sim 3 \times 10^7$ to 10^9 eV galactic cosmic ray electrons are still observed but their fluxes are attenuated and modulated. From a few hundred keV to a few MeV, electrons of Jovian origin dominate at quiet times. Below $\sim 10^2$ keV and down to $\lesssim 2$ keV it appears that the Sun is the dominant source at quiet times. We do not know the production mechanism for the quiet time 2–10^2 keV electrons from the Sun.

The active solar corona is continually accelerating electrons in coronal flares or small flare events which occur, on average, at least several times a day and sometimes, in type-III storms, much more frequently. These events are not known to be accompanied by detectable emissions of $\gtrsim 10$ MeV ions, but ions of lower energies, ~ 1 MeV nucl.$^{-1}$ or less, appear to be commonly accelerated in these small flares and coronal flares. These events preferentially accelerate ^{3}He.

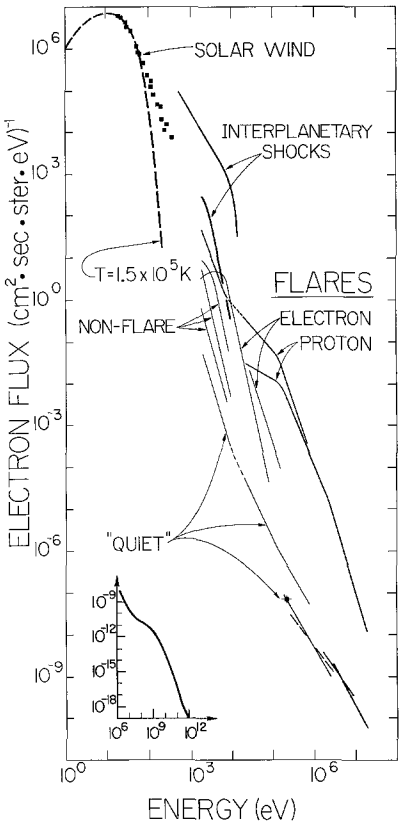

Fig. 18. A summary of the spectra of electrons observed in the interplanetary medium.

Large solar flares are characterized by a much different spectrum of accelerated electrons, which suggests a second acceleration stage occurs in these events. In addition large flares give rise to long-lived sources of low-energy electrons. In the absence of these long-lived streams, which dominate the observed interplanetary electrons in 1978–1979, there appears to be significant emission of 2–10^2 keV electrons by the Sun even at the quietest times.

The ISEE-3 particle and wave data have provided very illuminating measurements of the basic beam-plasma interaction which produce Langmuir waves and in turn, type-III radio emission. Although the basic ideas of Ginzburg and Zheleznyakov (1958) have been confirmed, these processes appear to be far more complicated. More detailed observations are required to provide a quantitative understanding of these plasma processes.

Acknowledgements

This research was supported in part by NASA grants NAG 5–376 and NGL-05–003–017.

References

Anderson, K. A. and Lin, R. P.: 1966, *Phys. Rev. Letters* **16**, 1121.
Anderson, K. A., Lin, R. P., Potter, D. W., and Heetderks, H. D.: 1977, *IEEE Trans.* **GE-16**, 153.
Anderson, K. A., McFadden, J. P., and Lin, R. P.: 1981, *Geophys. Res. Letters* **8**, 831.
Anderson, K. A., Lin, R. P., and Potter, D. W.: 1982, *Space Sci. Rev.* **32**, 169.
Bardwell, S. and Goldman, M. V.: 1976, *Astrophys. J.* **209**, 912.
Bohm, D. and Gross, E. P.: 1949, *Phys. Fluids* **75**, 1851.
Bougeret, J. L., Lin, R. P., Fainberg, J., and Stone, R. G.: 1985, *Astron. Astrophys.* (in press).
Chupp, E. L.: 1983, *Solar Phys.* **86**, 383.
Coplan, M. A., Ogilvie, K. W., Boschler, P., and Geiss, J.: 1983, *Solar Wind Five*, NASA CP-2280, p. 591.
Dulk, G. A., Steinberg, J. L., and Hoang, S.: 1985, *Astron. Astrophys.* (submitted).
Escande, L. A. and de Genouillac, G. V.: 1978, *Astron. Astrophys.* **68**, 405.
Fainberg, J. and Stone, R. G.: 1970, *Solar Phys.* **15**, 222.
Fainberg, J. and Stone, R. G.: 1974, *Space Sci. Rev.* **16**, 145.
Fainberg, J., Bougeret, J.-L., and Stone, R. G.: 1982, in M. Neugebauer (ed.), *Solar Wind Five*, NASA CP-2280, p. 469.
Feldman, W. C., Asbridge, J. R., Bame, S. J., Montgomery, M. D., and Gary, S. P.: 1975, *J. Geophys. Res.* **80**, 4181.
Fichtel, C. E. and McDonald, F. B.: 1967, *Ann. Rev. Astron. Astrophys.* **5**, 351.
Frank, L. A. and Gurnett, D. A.: 1972, *Solar Phys.* **27**, 448.
Frost, K. J. and Dennis, B. R.: 1971, *Astrophys. J.* **165**, 655.
Geiss, J. and Reeves, H.: 1972, *Astron. Astrophys.* **18**, 126.
Ginzburg, V. L. and Zheleznyakov: 1958, *Soviet Astron.* **AJ2**, 653.
Goldman, M. V.: 1983, *Solar Phys.* **80**, 403.
Goldman, M. V. and DuBois, D. G.: 1982, *Phys. Fluids* **25**, 1062.
Grognard, R. J.-M.: 1982, *Solar Phys.* **81**, 173.
Gurnett, D. A. and Anderson, R. R.: 1976, *Science* **194**, 1159.
Gurnett, D. A. and Anderson, R. R.: 1977, *J. Geophys. Res.* **82**, 632.
Hoyng, P.: 1975, Ph.D. Thesis, University of Utrecht, The Netherlands.
Hudson, H. S., Lin, R. P., and Stewart, R. T.: 1982, *Solar Phys.* **75**, 245.
Kaplan, S. A. and Tsytovich, V. N.: 1968, *Soviet Astron.-A.J.* **11**, 834.
Kellogg, P. J.: 1980, *Astrophys. J.* **236**, 696.
Lin, R. P.: 1970, *Solar Phys.* **12**, 266.
Lin, R. P.: 1974, *Space Sci. Rev.* **16**, 189.
Lin, R. P.: 1980, *Solar Phys.* **67**, 393.
Lin, R. P.: 1984, in S. E. Woosley (ed.), *High Energy Transients in Astrophysics*, American Inst. Phys., p. 619.
Lin, R. P., Evans, L. G., and Fainberg, J.: 1973, *Astrophys. Letters* **14**, 191.
Lin, R. P., Lotko, W., Gurnett, D. A., and Scarf, F. L.: 1985, *Astrophys. J.* (submitted).
Lin, R. P., Mewaldt, R. A., and Van Hollebeke, M. A. I.: 1982, *Astrophys. J.* **253**, 949.
Lin, R. P., Potter, D. W., Gurnett, D. A., and Scarf, F. L.: 1981, *Astrophys. J.* **251**, 364.
Lin, R. P., Schwartz, R. A., Kane, S. R., Pelling, R. M., and Hurley, K. C.: 1984, *Astrophys. J.* **283**, 421.
Magelssen, G. R., and Smith, D. G.: 1977, *Solar Phys.* **55**, 211.
Nicholson, D. R., Goldman, M. V., Hoyng, P., and Weatherall, J. C.: 1978, *Astrophys. J.* **225**, 605.
Papadopoulos, K., Goldstein, M. L., and Smith, R. A.: 1974, *Astrophys. J.* **190**, 175.
Pan, L. D., Lin, R. P., and Kane, S. R.: 1984, *Solar Phys.* **91**, 345.
Potter, D. W.: 1981, *J. Geophys. Res.* **86**, 111.
Potter, D. W., Lin, R. P., and Anderson, K. A.: 1980, *Astrophys. J. Letters* **236**, L97.
Ramaty, R., Kozlovsky, B., and Lingenfelter, R. E.: 1975, *Space Sci. Rev.* **18**, 341.
Ramaty, R., *et al.*: 1980, in P. A. Sturrock (ed.), *Solar Flares*, Colorado Associated University Press Boulder, Ch. 4, p. 117.
Reames, D. V., von Rosenvinge, T. T., and Lin, R. P.: 1985, *Astrophys. J.* **292**, 716.
Russell, D. A. and Goldman, M. V.: 1983, *Phys. Fluids* **26**, 2717.
Schwartz, R. A.: 1984, Ph.D. Thesis, University of California, Berkeley.
Simnett, G. M.: 1974, *Space Sci. Rev.* **16**, 257.
Steinberg, J. L., Dulk, G. A., Hoang, S., Lecacheux, A., and Aubier, M. G.: 1985, *Astron. Astrophys.* (submitted).

Sturrock, P. A.: 1964, in W. N. Hess (ed.), *AAS-NASA Symposium on the Physics of Solar Flares*, NASA SP-5, p. 357.
Takakura, T. and Shibahashi, H.: 1976, *Solar Phys.* **46**, 323.
Teegarden, B. J., McDonald, F. B., Trainor, J. H., Webber, W. R., and Roelof, E. C.: 1974, *J. Geophys. Res.* **79**, 3615.
Trubnikov, B. A.: 1965, *Rev. Plasma Phys.* **1**, 105.
Tsurutani, B. and Lin, R. P.: 1985, *J. Geophys. Res.* **90**, 1.
Tsytovich, V. N.: 1972, *Nonlinear Effects in Plasmas*, Plenum, New York.
Van Allen, J. A. and Krimigis, S. M.: 1965, *J. Geophys. Res.* **70**, 5737.
Van Hollebeke, M. A. I., MaSung, L. S., and McDonald, F. B.: 1975, *Solar Phys.* **41**, 189.
Zakharov, V. E.: 1972, *Soviet Phys. JETP* **35**, 908.